IJRRS
International Journal of Reliability, Risk Saftey: Theory and Application

Online ISSN: 2676-3346

OPEN ACCESS

Vol. 6/ Issue 2/ 2023/ pp. 27-35
DOI: 10.22034/IJRRS.6.2.4
Received: 11 September 2023, Accepted: 25 October 2023

Original Research Article

# Sensitivity Analysis of Flutter Velocity to Structural Properties of a Composite Wing

**Ali Bahrami Nejat[1], Mohammad Nadjafi[2] and Hossein Shahverdi[1]***

1- Department of Aerospace Engineering, Amirkabir University of Technology, Tehran, Iran

2- Aerospace Research Institute, Ministry of Science and Research, Tehran, Iran

*** h_shahverdi@aut.ac.ir**

**Abstract**

The main goal of this article is to analyze the sensitivity and find the most effective property among structural properties that have the most significant impact on the flutter velocity of a composite wing. For this purpose, the corresponding Aeroelastic equations of a composite wing have been derived using the Euler-Bernoulli beam model and discretized by the Galerkin method. Based on Jones's unsteady aerodynamic model, aerodynamic loads have been incorporated into the aeroelastic model. Then, flutter velocity was determined through eigenvalue analysis of the obtained aeroelastic equations. The Flutter velocity changes with a specific interval of each input. With the help of reverse engineering, the effects of structural properties (including material properties and effective stiffness) and their sensitivity were determined. The results show that the Torsional Effective Stiffness has the most significant effect and high sensitivity on flutter velocity. In this work, other parameters (including flow properties, wing geometry, and airfoil) are assumed to be unchangeable. The geometry of the wing is considered rectangular and straight.

**Keywords:** Wing Flutter; Composite Wing; Flutter Velocity Sensitivity Analysis; Jones aerodynamic model.

## Nomenclature

| | |
|---|---|
| $A$ | Wing section area |
| $b$ | Semi chord |
| $c$ | Chord |
| $C$ | Aeroelastic damping matrix |
| $\overline{EI}$ | Bending effective stiffness |
| $e$ | Distance between airfoil shear center and aerodynamic center |
| $G$ | Galerkin equation |
| $\overline{GJ}$ | Torsional effective stiffness |
| $I_{C.G}$ | Mass moment of inertia per unit length about the center of gravity |
| $I_\theta$ | Mass moment of inertia per unit length about the shear center |
| $i$ | General Counter |
| $K$ | Aeroelastic stiffness matrix |
| $K^*$ | Modified aeroelastic stiffness matrix |
| $\overline{K}$ | Bending-Torsional coupling effective stiffness |
| $L$ | Wing semi length |
| $\bar{L}$ | Lift per unit length |
| $\bar{L}_c$ | Circulatory lift |
| $\bar{L}_{n.c}$ | Non-Circulatory lift |
| $M$ | Aeroelastic mass matrix |
| $M^*$ | Modified aeroelastic mass matrix |
| $M_{A.C}$ | Bending moment about aerodynamic center |
| $M_{s.c}$ | Bending moment about shear center |
| $m$ | Mass per unit length |
| $N$ | Modes total number |
| $r$ | Distance between a point and centroid |
| $R_\Omega$ | Residual values of differential equation in the Galerkin method |
| $S_\theta$ | Mass unbalance per unit length |
| $t$ | Time |
| $u$ | Flow velocity |
| $u_f$ | Flutter velocity |
| $w$ | Wing deflection |
| $W_{3c/4}$ | Vertical component of flow velocity in ¾ of chord |
| $x_\theta$ | Dimensionless distance between mass center and shear center in airfoil |
| $y$ | Wing axis |
| $\bar{\alpha}_i$ | Bending assumed mode constant |
| $\beta_i$ | Constant |
| $\bar{\beta}_i$ | Bending assumed mode constant |
| $\gamma_1$ | Constant |
| $\bar{\gamma}_i$ | Torsional assumed mode constant |
| $\eta_i$ | Bending assumed mode coefficient |
| $\theta_i$ | Torsional assumed mode |
| $\theta$ | Wing torsion |
| $\lambda_i$ | Jones variable |
| $\xi$ | Unknown matrix |
| $\rho_s$ | Structural density |
| $\Phi_i$ | General mode in the Galerkin method |
| $\phi$ | Torsional assumed mode coefficient |
| $\psi$ | Bending assumed mode |
| $\Omega$ | Problem boundaries |
| $\omega_f$ | Flutter frequency |

**How to cite this article:**

A. Bahrami Nejat, M. Nadjafi and H. Shahverdi. "Sensitivity Analysis of Flutter Velocity to Structural Properties of a Composite Wing," *International Journal of Reliability, Risk and Safety: Theory and Application*, vol. 6, no. 2, pp. 27-35, 2023.

# 1. Introduction

Aeroelasticity is one of the engineering branches that studies the interaction of structural, aerodynamic, and inertial forces in flexible structures. The field of static aeroelasticity studies the interaction of aerodynamic loading induced by steady flow and the resulting elastic deformation of the lifting surface structure. On the other hand, dynamic aeroelasticity is the field of aeroelasticity that investigates the combined effects of inertial and aerodynamic forces on a flying object's deformation [1]. The schematic interactions of these forces are shown in **Figure 1**.

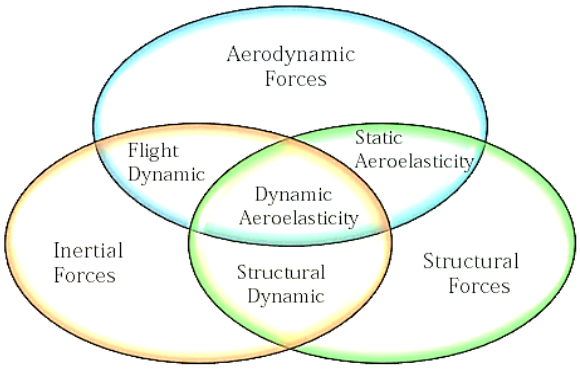


**Figure 1.** Interactions of Aeroelastic forces [1]

The interaction of the three forces above can cause several undesirable phenomena. These phenomena include flutter, divergence, control reversal, and so on. Hence, this paper focuses on the flutter phenomenon; this issue has been further studied and investigated. Flutter is a dynamic instability of a flight vehicle associated with the interaction of aerodynamic, elastic, and inertial forces. Based on this definition, it is apparent that any investigation of flutter stability requires adequate system knowledge of structural dynamic and aerodynamic properties. To further elaborate, flutter is a self-excited and potentially destructive oscillatory instability in which aerodynamic forces on a flexible body are coupled with its natural vibration modes to produce oscillatory motions with dramatically increasing amplitude of linear aeroelastic systems [2,3]. Flutter testing is critical to the envelope expansion for any new airplane. Until the testing is complete, flight test aircraft may be limited to certain speeds, altitudes, and weights during various maneuvers. During the flutter testing flights, pilots introduce a range of vibration frequencies to the flight surfaces and flight control surfaces to ensure the design of the aircraft dampens out the oscillations without further input from the pilots. These oscillations are introduced by hand as well as via computer. Flight flutter tests are done at different stages of aircraft manufacturing. An aircraft is primarily designed with software and theoretical equations to reduce cost. The flutter phenomena under different conditions are investigated. The advantage of calculating flutter velocity and frequency before manufacturing is that the order of flutter velocity and frequency for primary design is obtained in this stage. Then, based on this data, the aircraft shape is optimized to have better behavior in dealing with the flutter phenomenon [4].

The flutter on the wings is one of the significant problems in aircraft. In the conceptual and primary design stages, having an accurate wing model with complete equations can lead to better prediction of flutter phenomena. Furthermore, considering uncertain conditions can help to have a better prediction about flutter velocity and frequency limit. Aeroelastic instabilities take place when an elastic wing is exposed to airflow. A wind tunnel test or theoretical analysis with experimentally obtained parameters can predict this phenomenon. Flutter velocity is an important criterion for the dynamic instability of aeroelastic wings. Most parameters involved in flutter prediction are physically uncertain variables; conducting a reliability analysis to determine the wing flutter boundary would make more sense. Indeed, it is more practical to define the possibility of flutter occurrence on an airspeed range than to state a critical wind speed as a flutter boundary.

# 2. Literature review

Determining the flutter instability of aircraft wings has been a challenge for aeronautical engineering for many years. In this regard, some research has been conducted to analyze and determine the characteristics of this phenomenon utilizing a cantilever clean wing [5], the mathematical analysis [6], the flutter investigation of a wing with tip weights [7, 8], the flutter of a forward-swept wing with tip weights [9], efforts to show the effects of externally mounted masses on the static and dynamic aeroelasticity of advanced swept cantilevered wings [10], the effect of thrust on the flutter [11], the dynamic aeroelastic response and the related control [12], the nonlinear aeroelastic and sensitivity analysis of high aspect ratio wings [13], the numerical modeling of the flutter problem of viscoelastic plate [14], the supersonic flutter on composite panels [15], and so on.

# 3. Deterministic Aeroelastic Wing Flutter Modeling/ Governing Equations

Based on references [1,16], consider a rectangular straight composite wing of chord $c$ and length $L$ that exhibits both geometric and material coupling. The flow field passes around the wing with velocity $u$. The schematic of wing is shown in **Figure 2**.

The elastic axis, which coincides with the y-axis, is chosen to be the locus of the geometric shear centers of the wing cross-section. It also shows the spanwise coordinate on the wing. Wing cross-section is allowed to deflect out of the plane by $w_{(y,t)}$ and also is allowed to rotate about the y-axis by $\theta_{(y,t)}$ where y and t denote the

spatial and time coordinates, respectively. Eq. (1) and (2) give the governing differential equations of composite wing airfoil.

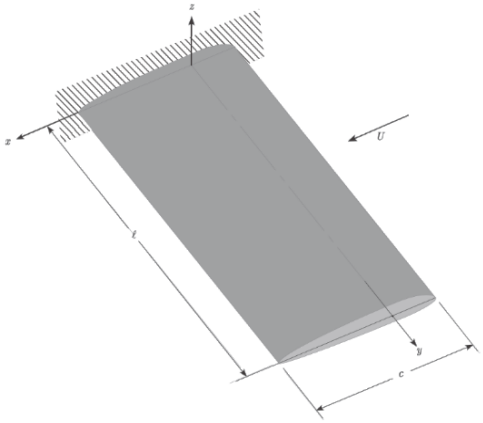

**Figure 2.** Schematic of the rectangular straight wing [1]

$$m\ddot{w} - S_\theta\ddot{\theta} + \bar{K}\theta''' + \overline{EI}w^{(4)} = \bar{L} \quad (1)$$

$$-S_\theta\ddot{w} + I_\theta\ddot{\theta} - \bar{K}w''' - \overline{GJ}\theta'' = M_{s.c} \quad (2)$$

The wing has effective bending stiffness ($\overline{EI}$), torsional effective stiffness ($\overline{GJ}$), bending–torsional coupling effective stiffness ($\bar{K}$), mass per unit length $m$, mass moment of inertia per unit length $I_\theta$ about the shear center ($I_\theta = I_{C.G} + m(bx_\theta)^2$) and mass unbalance per unit length $S_\theta$ ($S_\theta = mbx_\theta$), respectively. In the wing cross-section, $b$ is semi-chord ($b = \frac{c}{2}$) and $x_\theta$ is the dimensionless distance between the mass center (C.G) and the shear center (S.C), respectively. The two principal parameters that are responsible for the geometric and material coupling are $x_\theta$ and $\bar{K}$, respectively.

On the right-hand side of Eq. (1) and (2), $\bar{L}$ and $M_{s.c}$ denotes aerodynamics lifting force and bending moment about the shear center, respectively. In this article, $\bar{L}$ and $M_{s.c}$ are defined by Jones's unsteady aerodynamic model. This model applies to thin airfoils and flat plates. This model assumed that lifting force consists of circulatory lift ($\bar{L}_c$), and non-circulatory lift ($\bar{L}_{n.c}$). $\bar{L}_{n.c}$ and $M_{A.C}$ ($M_{s.c} = M_{A.C} + e \times \bar{L}$) which is the bending moment about the aerodynamic center are functions of $w$ and $\theta$, and $\bar{L}_c$ is defined by improving on Theodorson's aerodynamic model. Theodorson model applies only to oscillatory airfoils and $\bar{L}_c$ will be a function of time and frequency in this model. During Jones's improvement, by using both Fourier transform and inverse Fourier transform on $\bar{L}_{n.c}$, the term of frequency has been deleted, and the new expression of $\bar{L}_c$ is a function of only time, and the new $\bar{L}_c$ can be used for any desired movement, not only oscillatory movement. Jones's unsteady aerodynamic model is a state space form of Wagner`s aerodynamic model, which provides an eigenvalue form of the aeroelastic equations. The final relations of aerodynamics lifting force and bending moment of airfoil are presented in Eq. (3) to Eq. (7).

$$M_{c/4} = -\pi\rho b^3\left[\frac{-\ddot{w}}{2} + u\dot{\theta} + b(\frac{1}{8} - \frac{a}{2})\ddot{\theta}\right] \quad (3)$$

$$L_{N.c} = \pi\rho b^2\left[-\ddot{w} + u\dot{\theta} - ba\ddot{\theta}\right] \quad (4)$$

$$L_c = \pi\rho uc\left[{}^1\!/_2 \times W_{3c/4} + \gamma_1\lambda_1 + \gamma_2\lambda_2\right] \quad (5)$$

$$W_{3c/4} = -\dot{w} + u\theta + b(\frac{1}{2} - a)\dot{\theta} \quad (6)$$

$$\dot{\lambda}_i + \beta_i\frac{u}{b}\lambda_i = W_{3c/4} \quad i = 1,2 \quad (7)$$

In the above equations, $W_{3c/4}$ is the vertical component of flow velocity in ${}^3\!/_4$ of chord, which is defined in Eq. (6) as a function of $w$ and $\theta$. $\beta_i$ and $\gamma_i$ are constants, and they are defined in [1]. $\lambda_i$ is called Jones variable and can be calculated by solving Eq. (7). But the Eq. (7). Is coupled with Eq. (1) and (2) and there isn't any close form solution for them. They will be solved by a P-method numerical solution.

Eq. (1) and (2) are derived for a differential segment of a composite wing; the present study uses the Galerkin method to drive wing equations. In this method, the degrees of freedom are assumed as an infinite series of assumed modes, as shown in Eq. (8) and (9) for $w$ and $\theta$, respectively.

$$w_{(t,y)} = \sum_{i=1}^{N}\eta_i\psi_i \quad (8)$$

$$\theta_{(t,y)} = \sum_{i=1}^{N}\phi_i\Theta_i \quad (9)$$

In Eq. (8) and (9), the terms $\psi$ and $\Theta$ are bending and torsion assumed modes, respectively, and both are functions of y. The expressions for this assumed mode have been shown in Eq. (10) and (11). In these equations $\bar{\alpha}_i$, $\bar{\beta}_i$ and $\bar{\gamma}_i$ are all constants [1].

$$\psi_{i_{(y)}} = cosh(\bar{\alpha}_i y) - cos(\bar{\alpha}_i y) - \bar{\beta}_i[sinh(\bar{\alpha}_i y) - sin(\bar{\alpha}_i y)] \quad (10)$$

$$\Theta_i = \sqrt{2}\,sin(\bar{\gamma}_i y) \quad (11)$$

In the above equations, the terms $\eta_i$ and $\phi_i$ are bending and torsion unknown coefficients, respectively, which are time functions. $N$ is the counter of series in both Eq. (8) and (9). In general, the counter of two series can be different, but in this work, they are equal. By checking the convergences of series, it is possible to use a finite number of series $N$.

The Galerkin general equation $G_i$ has been expressed in Eq. (12). $\Phi_i$ is the general form of assumed mode and $R_\Omega$ is residual of the differential equation after replacing the unknown variable with the assumed series [17].

$$G_i: \int R_\Omega\Phi_i d\Omega = 0 \quad i = 1, \dots, N \quad (12)$$

Because of using $N$ mode(s), there will be $N$ Galerkin equation(s) and $N$ unknown coefficient(s). So, this system of linear equations can be solved to find the unknown coefficient (s).

In the flutter phenomenon, the Galerkin equations are coupled (because of the coupling between aerodynamics and structure), and there is no closed-form solution. Instead, the equations can be solved with numerical methods like P-method. In this method, all equations are arranged in matrix form, the same as Eq. (13).

$$M\ddot{\xi} + C\dot{\xi} + K\xi = 0 \quad (13)$$

In Eq. (13), the term $\xi$ is a general form of an unknown matrix, and $M$, $C$ and $K$, are aeroelastic mass, damping, and stiffness matrices, respectively. P-method will use the solution of the eigenvalue problem, so the three coefficient matrixes of Eq. (13) have to be reduced to two coefficient matrices: $M^*$ and $K^*$, as follows.

$$M^* = \begin{bmatrix} [I] & [0] \\ [0] & M \end{bmatrix}$$
$$K^* = \begin{bmatrix} [0] & -[I] \\ K & C \end{bmatrix} \quad (14)$$

$$M^*\dot{\xi}^* + K^*\xi^* = 0, \xi^* = \begin{bmatrix} \xi \\ \dot{\xi} \end{bmatrix} \quad (15)$$

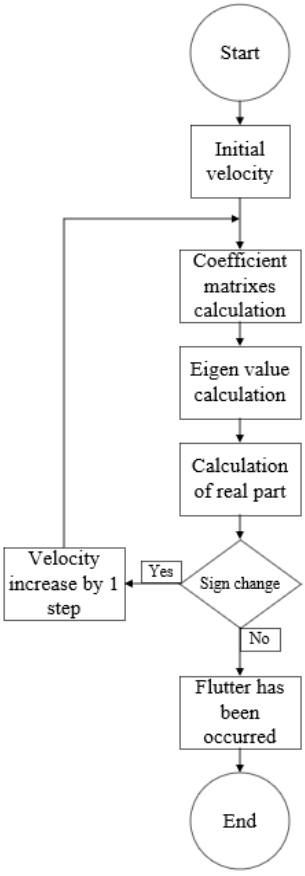


**Figure 3.** Flowchart of P-method

In Eq. (14), $[0]$ and $[I]$ are zero and identity matrix, respectively. The P-method will solve Eq. (15) and define the eigenvalues of $-M^{*-1}K^*$ matrix. The eigenvalues are complex numbers, and the occurrence of flutter will cause a change in the sign of the real part of at least one couple of eigenvalues. The flowchart using the P-method has been shown in **Figure 3**. As has been seen in **Figure 3**, for founding flutter velocity, an initial velocity is selected, and the quantity of $-M^{*-1}K^*$ is calculated based on velocity and other parameters, and then eigenvalues can be calculated. If there were no changes in the real part of eigenvalues, velocity can increase by one step, and eigenvalues can be calculated for new velocities. The process will continue until the sign changes in the real part of any couple of eigenvalues and the flutter has occurred at this velocity. The absolute imaginary part of eigenvalues is the frequency of flutter.

# 4. Validation of Equations

For validation, the results of the equations of this research have been compared with reference [18]. This reference calculated the flutter velocity and frequency of a specific problem. This reference considered a rectangular straight composite wing with 9 different cases of composite layering. The input parameters based on the reference are listed in **Table 1**, details of layering per each case are listed in **Table 2**, and the results of calculating effective stiffnesses and flutter velocity and frequency per case are listed in **Table 3**.

**Table 1.** Fix inputs

| Parameter | Quantity | Unit |
|---|---|---|
| Flow density | 1.225 | $Kg/m^3$ |
| Semi wing length | 0.55 | $m$ |
| Airfoil chord | 0.1 | $m$ |
| Distance between airfoil C.G. and S.C | 9.5 | $mm$ |
| Distance between mid-airfoil and A.C | -0.39 | Dimensionless |
| mass per unit length | 0.68 | $Kg/m$ |
| mass moment of inertia per unit length | $2.75\times10^{-4}$ | $Kg.m^2/m$ |

**Table 2.** Layering per each case

| Case | layering |
|---|---|
| 1 | $[-20_8]$ |
| 2 | $[0/30/30/0]_s$ |
| 3 | $[45/0/45/0]_s$ |
| 4 | $[0/45/0/45]_s$ |
| 5 | $[-25_8]$ |
| 6 | $[45/-45/45/-45]_s$ |
| 7 | $[45/30/45/-45]_s$ |
| 8 | $[45/-45/45/-30]_s$ |
| 9 | $[45/-45/45/30]_s$ |

**Table 3.** Effective stiffnesses, flutter velocity, and frequency per each case of layering

| Case | Effective stiffnesses | Flutter velocity and frequency |
|---|---|---|
| 1 | $\overline{EI} = 3.296$<br>$\overline{K} = 1.349$<br>$\overline{GJ} = 4.202$ | $u_f = 67.85$<br>$\omega_f = 134$ |
| 2 | $\overline{EI} = 3.475$<br>$\overline{K} = -0.466$<br>$\overline{GJ} = 4.018$ | $u_f = 70$<br>$\omega_f = 182.5$ |
| 3 | $\overline{EI} = 2.785$<br>$\overline{K} = 0$<br>$\overline{GJ} = 5.748$ | $u_f = 87$<br>$\omega_f = 186.65$ |
| 4 | $\overline{EI} = 3.463$<br>$\overline{K} = 0$<br>$\overline{GJ} = 4.094$ | $u_f = 71$<br>$\omega_f = 183.57$ |
| 5 | $\overline{EI} = 2.983$<br>$\overline{K} = 1.427$<br>$\overline{GJ} = 4.948$ | $u_f = 72.742$<br>$\omega_f = 125.07$ |
| 6 | $\overline{EI} = 2.070$<br>$\overline{K} = 0$<br>$\overline{GJ} = 7.127$ | $u_f = 99$<br>$\omega_f = 197$ |
| 7 | $\overline{EI} = 2.255$<br>$\overline{K} = -0.420$<br>$\overline{GJ} = 6.772$ | $u_f = 99.286$<br>$\omega_f = 192.55$ |
| 8 | $\overline{EI} = 2.080$<br>$\overline{K} = 0.022$<br>$\overline{GJ} = 7.109$ | $u_f = 98.88$<br>$\omega_f = 195.83$ |
| 9 | $\overline{EI} = 2.080$<br>$\overline{K} = -0.022$<br>$\overline{GJ} = 7.109$ | $u_f = 101.88$<br>$\omega_f = 195.13$ |

In **Table 4** and **Table 5**, the results of the flutter velocity calculation according to the equations of the previous section and the error of calculation compared to the flutter velocity in **Table 3** are listed for $N = 1$ and $N = 2$, respectively.

Due to Eq. (8) and (9), the convergence of flutter velocity by increasing $N$ must be checked. For these purposes, in this article, a maximum error of 5% has been chosen, and an increase of $N$ will continue until the errors of all calculated velocities are less than 5%. The errors of calculation are shown in **Figure 4**.

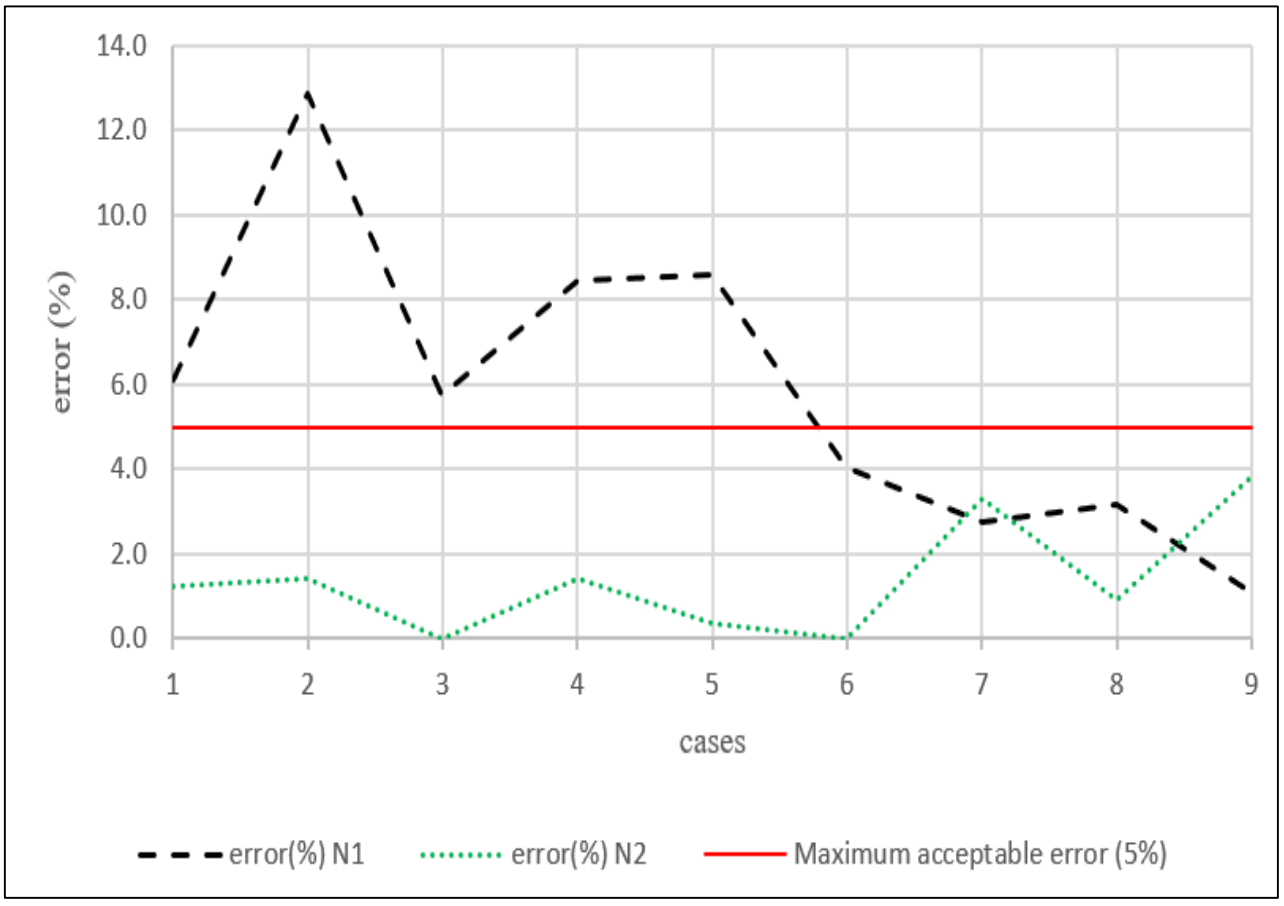


**Figure 4.** Error of calculation

**Table 4.** Calculated flutter velocity and its error for $N = 1$

| Case | Calculated Flutter Velocity (m/s) | Calculation Error (%) |
|---|---|---|
| 1 | 72 | 6.1 |
| 2 | 79 | 12.9 |
| 3 | 92 | 5.7 |
| 4 | 77 | 8.5 |
| 5 | 79 | 8.6 |
| 6 | 103 | 4.0 |
| 7 | 102 | 2.7 |
| 8 | 102 | 3.2 |
| 9 | 103 | 1.1 |

**Table 5.** Calculated flutter velocity and its error for $N = 2$

| Case | Calculated Flutter Velocity (m/s) | Calculation Error (%) |
|---|---|---|
| 1 | 67 | 1.3 |
| 2 | 69 | 1.4 |
| 3 | 87 | 0.0 |
| 4 | 70 | 1.4 |
| 5 | 73 | 0.4 |
| 6 | 99 | 0.0 |
| 7 | 96 | 3.3 |
| 8 | 98 | 0.9 |
| 9 | 98 | 3.8 |

As shown in Figure 4, the errors of calculated velocity for $N = 1$ (black dash) in five cases are greater than 5%, and it is not acceptable. Still, errors of calculated velocity for $N = 2$ (green dot) in all cases are less than 5% (even less than 4%), and so using only 2 terms in Eq. (8) and (9) is enough. The calculation also shows that the average calculated velocity error in the case of choosing $N = 2$ is about 1.4% and so the calculation based on equations of the previous section is valid. Now, it is possible to calculate the flutter velocity based on the modeling of the previous section and input data.

# 5. An Approach to Sensitivity Analysis

Understanding the effect of a particular assumption on model predictions is often informative and valuable. The impact of using alternative assumptions or models may be addressed by performing appropriate sensitivity studies or using qualitative reasoning. This may be part of the assessment of model uncertainty. Sensitivity analysis can be performed to identify the dominant factors in system uncertainty. System performance can then be improved by reducing sources of human error or redesign.

The basic steps that can be used for sensitivity analysis are given in the diagram in **Figure 5**.

In the first step, an analysis model must be defined. This may depend on the condition of the problem and the required accuracy. Based on this, the elements of analysis are identified. These include the problem assumptions, sensitive parameters, variable inputs, and physical models considered. Models depend on the nature of the problem. It can be a purely theoretical model based on mathematical descriptions or a numerical model, depending on the complexity of the physical properties.

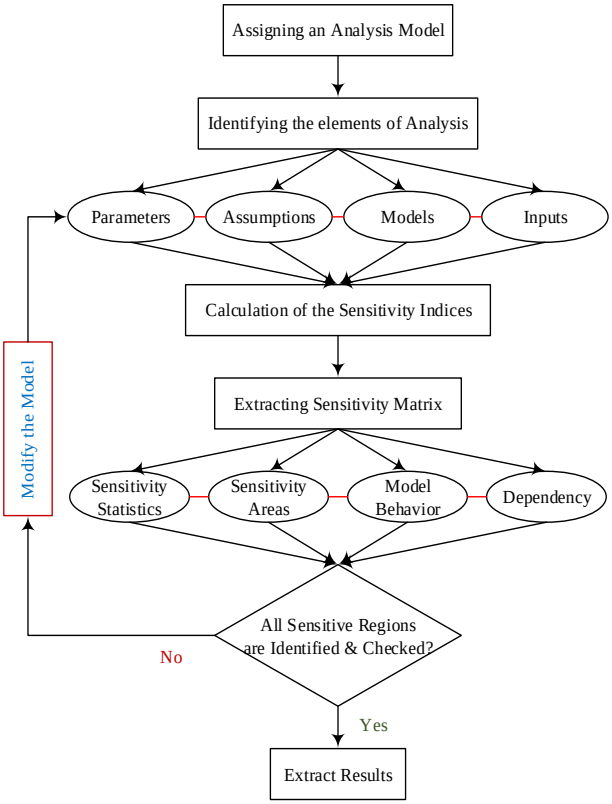


**Figure 5.** Main steps of sensitivity analysis

Next, sensitivity indices are calculated, and matrices are extracted. These reveal the relative importance and classification of parameters (sensitivities statistics) and their sensitive regions, unusual behavior of the probabilistic model, and parameter dependence (through correlation and regression analysis, if needed) [19, 20].

Initial sensitivity analysis studies can focus on two things:

- Detailed results to guide research and aid model development efforts and
- Calculate general descriptions of uncertainty associated with model predictions so that decisions can reflect the predicted performance of the system and accuracy.

The sensitivity analysis results may be used to identify areas where more data collection and better analysis are needed (e.g., using higher and more accurate techniques and models) [21]. According to the flowchart in **Figure 5**, after checking and identifying the acceptable ranges of the results, if the results are not within the acceptable range, corrective changes should be applied to

the system, and the results should be recalculated. Sensitivity analysis can be performed to identify the factors that dominate the system's unreliability. It should be noted that reducing sources of human error or redesigning protection systems can improve system performance. The accuracy and reliability of the output indicate the desirability of a model. Studying the outputs of the uncertainty of an output parameter resulting from the modeling, analysis, and simulation of a system and obtaining different sources of uncertainty in the input variables is one of the achievements of the study of sensitivity analysis [22].

## 6. Sensitivity Analysis of Structural properties on Flutter velocity

According to the contents of the Aeroelastic wing flutter equations, Eq. (13) governs the wing flutter problem. Still, of course, only two equations are defined in the wing section, as described before. In terms of the increase of variables in converting the equations of the wing section to the equations of the wing using the Galerkin method, only the geometrical parameters have been added to the final matrices (in this article, only wing length, L), which are assume unchangeable. Also, on the right-hand side of wing section equations, there are only aerodynamic parameters; in this article, the sensitivity of velocity to these parameters is not considered.

By examining the left-hand side of wing section equations, it is clear that 6 structural parameters are known as $m$, $S_\theta$, $I_\theta$, $\overline{EI}$, $\overline{K}$, and $\overline{GJ}$. Of course, these parameters can be classified into two general categories: the structure's mass properties and effective stiffness properties. The two parameters $S_\theta$ and $I_\theta$ somehow indicate the distribution of the mass in the wing cross-section and are functions of the mass and geometry of the airfoil. Based on the assumption that the geometry of the wing is certain, the airfoil is assumed to fix, and as a result, $S_\theta$ and $I_\theta$ parameters are considered as the only mass function. The cross-sectional mass of the wing itself can be considered a function of the wing density (assuming to define a uniform density for the wing). In this way, all three mass properties are obtained as a function of the wing density, $\rho_s$, which is shown in Eq. (16) to (20).

$$m = \rho_s \times A \Rightarrow dm = \rho_s \times dA \quad (16)$$

$$S_\theta = bx_\theta m = \rho_s \times bx_\theta A \quad (17)$$

$$I_\theta = I_{C.G} + m(bx_\theta)^2, I_{C.G} = \iint_A r^2 dm \quad (18)$$

$$I_\theta = \iint_A r^2 \rho_s \times dA + \rho_s \times A(bx_\theta)^2 \quad (19)$$

$$I_\theta = \rho_s \times \left(\iint_A r^2 dA + A(bx_\theta)^2\right) \quad (20)$$

As can be seen in Eq. (16) to (20), all three mass properties $m$, $S_\theta$ and $I_\theta$ are equal to the structural density $\rho_s$ times, some other geometrical parameters are not considered in this work, so the sensitivity of flutter velocity, instead of all three mass properties, has only been analyzed to structural density.

## 7. Results and Discussion

In this article, the sensitivity of flutter velocity has been analyzed to four parameters $\overline{EI}$, $\overline{K}$, $\overline{GJ}$ and $\rho_s$ individually. For each case of layering, $\overline{EI}$, $\overline{K}$, $\overline{GJ}$ and $\rho_s$ increases and decreases by 10% individually, and flutter velocity changes due to changes in the above parameters are calculated. An average is taken for each case of layering between absolute changes in flutter velocity due to the increasing and decreasing of one specific parameter. It is important to emphasize that there is no need to calculate $\rho_s$, and in calculations that require changing $\pm 10\%$ in $\rho_s$, the three mass properties $m$, $S_\theta$ and $I_\theta$ can change $\pm 10\%$ all together. The results are shown in **Figure 6**.

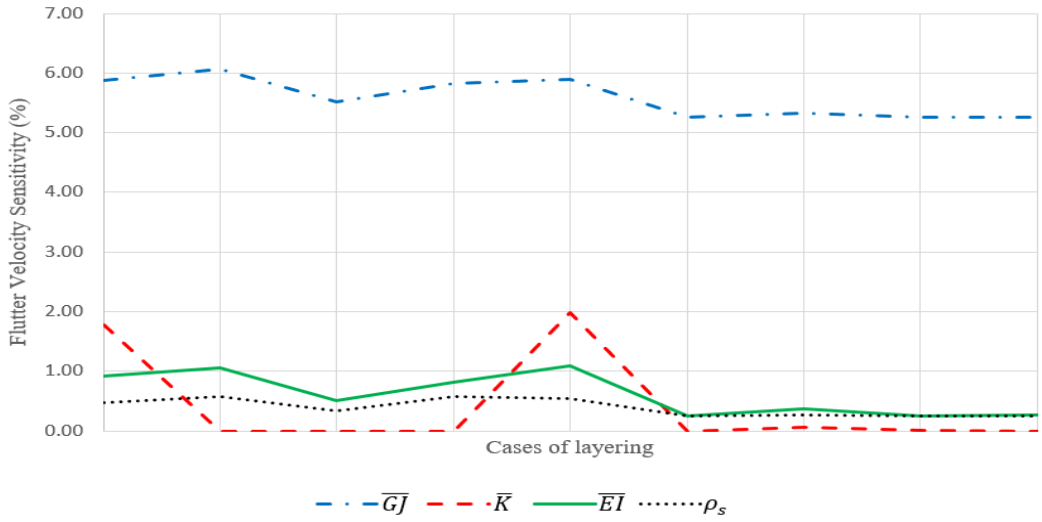


**Figure 6.** Flutter Velocity Sensitivity

As is evident in **Figure 6**, changes in the torsional effective stiffness $\overline{GJ}$ has the most effect on changing flutter velocity in all cases of layering, or somehow, it can be said flutter velocity has the most sensitivity to $\overline{GJ}$ among all investigated structural parameters.

The order of flutter velocity sensitivity to other parameters is unclear in **Figure 6**, and it changes in each case of layering.

**Table 6** clears the Order of flutter velocity sensitivity to structural parameters. In this table for each parameter, an average has been taken among the 9 cases of layering (second column), and parameters have been sorted decreasing due to the average effect on flutter velocity. Because of the small effect of some parameters on flutter velocity, the initial change of parameter has been chosen as 10%, although it is expected to choose 1% for the initial change. In the last column, the average effect (second column) is divided into initial change (10%), and the average effect without the initial effect has been calculated. The last column somehow shows each parameter's uncertainty of flutter velocity separately. Even though calculating the uncertainty in this way is very superficial, there are more precise methods of uncertainty calculation that are beyond the scope of this article.

**Table 6.** Order of flutter velocity sensitivity to structural parameters

| Parameter | Average effect (%) | Average effect without initial effect |
|---|---|---|
| $\overline{GJ}$ | 5.59 | 0.56 |
| $\overline{EI}$ | 0.62 | 0.06 |
| $\overline{K}$ | 0.42 | 0.04 |
| $\rho_s$ | 0.39 | 0.04 |

Two points are left about **Table 6**. The first point is that in calculating the average effect of $\overline{K}$, this parameter is equal to zero in many cases (see **Table 3**) and does not affect flutter velocity. So, this data has an attenuating effect on the average effect of $\overline{K}$ on flutter velocity. Also, in some other case although $\overline{K}$ is not equal to zero, but it is 2 order smaller than $\overline{EI}$ and so making change in $\overline{K}$ has small effect on flutter velocity. Based on these points, it is hard to say certainly that $\overline{EI}$ has more effect than $\overline{K}$ on flutter velocity. As you can see in **Figure 6** in cases 1 and 5 of layering, $\overline{K}$ has greater effect than $\overline{EI}$ although $\overline{K}$ is 1 order smaller than $\overline{EI}$.

The second point about **Table 6** is about $\rho_s$. In case of changing $\rho_s$, all mass properties are changing together, and if it were possible to separate their effects, the average effect of each mass parameter would be much smaller than now. With all this, the important extracted information is that $\overline{GJ}$ has the most effect on flutter velocity among structural parameters.

# Conclusion

In this article, a brief study of flutter and its governing equations has been done, and the equations have been validated. After that, a brief study about sensitivity analysis was done, and the sensitivity of flutter velocity to structural properties was investigated.

The results show that effective torsional stiffness ($\overline{GJ}$) has the most effect on flutter velocity and structural density ($\rho_s$) has the least effect (except the cases with $\overline{K} = 0$). The other parameters $\overline{EI}$ and $\overline{K}$ effects are between $\overline{GJ}$ and $\rho_s$ (except the cases with $\overline{K} = 0$), but their order depends on their value and can change case by case.

On the other hand, the 9 cases of layering are divided into two groups. The first group, which all have $\overline{K} = 0$ (cases 3,4 and 6), and the second group, which all have $\overline{K} \neq 0$. In the first group, $\overline{GJ}$ has the most effect, after that $\overline{EI}$, and at last $\rho_s$ has the least effect, and the study of $\overline{K}$ effect is meaningless. In the second group, steel $\overline{GJ}$ has the most and $\rho_s$ has the least effect and $\overline{EI}$ and $\overline{K}$ effects are between $\overline{GJ}$ and $\rho_s$, hence, their order is not predictable.

For future work, the sensitivity of flutter velocity to other parameters like geometric or aerodynamic parameters can be investigated. The results of this article can be used in defining and controlling flutter velocity in designing a wing. Also, the extracted results can be used in uncertainty analysis of flutter velocity due to the uncertainty of structural properties during simulation methods such as the Mont Carlo or Markov chain.

# 8. References

[1] D. H. Hodges and G. A. Pierce, Introduction to structural dynamics and aeroelasticity, vol. 15. Cambridge University Press, 2011.

[2] T. Theodorsen and I. Garrick, Mechanism of flutter: a theoretical and experimental investigation of the flutter problem vol. 685: NACA Langley Field, VA, USA, 1940.

[3] I. Garrick and W. H. Reed III, "Historical development of aircraft flutter," Journal of Aircraft, vol. 18, no. 11, pp. 897-912, 1981. doi: https://doi.org/10.2514/3.57579.

[4] Y. Watanabe, S. Suzuki, M. Sugihara, and Y. Sueoka, "An experimental study of paper flutter," Journal of Fluids and Structures, vol. 16, no. 4, pp. 529-542, 2002. doi: https://doi.org/10.1006/jfls.2001.0435.

[5] M. Goland, "The Flutter of a Uniform Cantilever Wing," Journal of Applied Mechanics, vol. 12, no. 4, pp. A197-A208, 2021, doi: https://doi.org/10.1115/1.4009489.

[6] M. A. Shubov, "Flutter phenomenon in aeroelasticity and its mathematical analysis," Journal of Aerospace Engineering, vol. 19, no. 1, pp. 1-12, 2006. doi:

https://doi.org/10.1061/(ASCE)0893-1321(2006)19:1(1)
[7] M. Goland and Y. Luke, "The flutter of a uniform wing with tip weights," 1948.
[8] H. L. Runyan and C. E. Watkins, "Flutter of a uniform wing with an arbitrarily placed mass according to a differential-equation analysis and a comparison with experiment," 1949.
[9] I. Lottati, "Flutter and divergence aeroelastic characteristics for composite forward swept cantilevered wing," Journal of Aircraft, vol. 22, no. 11, pp. 1001-1007, 1985. doi: https://doi.org/10.2514/3.45238.
[10] F. H. Gern and L. Librescu, "Effects of externally mounted stores on aeroelasticity of advanced swept cantilevered aircraft wings," Aerospace science and technology, vol. 2, no. 5, pp. 321-333, 1998. doi: https://doi.org/10.1016/S1270-9638(98)80008-4.
[11] D. H. Hodges, M. J. Patil, and S. Chae, "Effect of thrust on bending-torsion flutter of wings," Journal of Aircraft, vol. 39, no. 2, pp. 371-376, 2002. doi: https://doi.org/10.2514/2.2937.
[12] L. Librescu and O. Song, Thin-walled composite beams: theory and application vol. 131. Springer Science & Business Media, 2005.
[13] E. Zafari, M. Jalili, and A. Mazidi, "Analytical nonlinear flutter and sensitivity analysis of aircraft wings subjected to a transverse follower force," Proceedings of the Institution of Mechanical Engineers, Part G: Journal of Aerospace Engineering, vol. 233, no. 4, pp. 1503-1515, 2019. doi: https://doi.org/10.1177/0954410017754171.
[14] B. Khudayarov, F. Z. Turaev, K. Ruzmetov, and A. Tukhtaboev, "Numerical modeling of the flutter problem of viscoelastic elongated plate," in AIP Conference Proceedings, 2012, vol. 2402, no. 1. AIP Publishing. doi: http://dx.doi.org/10.1063/5.0071353.
[15] T. A. Guimarães, F. D. Marques, and A. J. Ferreira, "On the modeling of nonlinear supersonic flutter of multibay composite panels," Composite Structures, vol. 232, p. 111522, 2020. doi: https://doi.org/10.1016/j.compstruct.2019.111522.
[16] E. H. Dowell, A modern course in aeroelasticity vol. 217. Springer, 2014.
[17] D. L. Logan, First Course in the Finite Element Method, Enhanced Edition, SI Version: Cengage Learning, 2022.
[18] A. A. A.-H. Ali and M. I. Hamed, "The effect of laminated layers on the flutter speed of composite wing," Journal of Engineering, vol. 18, no. 08, pp. 924-934, 2012, [Online]. Available: https://www.iasj.net/iasj/download/ac9106d5ba8c32be
[19] M. Modarres, M. P. Kaminskiy, and V. Krivtsov, Reliability engineering and risk analysis: a practical guide: CRC Press, 2016.
[20] M. Talafi Noghani and M. Nadjafi, "Thermal Sensitivity Analysis of a Telemetry Antenna in Sub-Orbital Spaceflights," International Journal of Reliability, Risk and Safety: Theory and Application, vol. 4, no. 2, pp. 13-19, 2021. doi: https://doi.org/10.30699/IJRRS.4.2.2.
[21] R. Teja Nallapu and J. Thangavelautham, "Design and sensitivity analysis of spacecraft swarms for planetary moon reconnaissance through co-orbits," Acta Astronautica, vol. 178, pp. 854-869, 2021. doi: https://doi.org/10.1016/j.actaastro.2020.10.008.
[22] M. Nadjafi, M. Farsi, and F. Ommi, "Uncertainty analysis of spray injection process in a model scale liquid fuel micro-motor," *Iranian Journal of Mechanical Engineering Transactions of the ISME*, vol. 21, no. 2, 2020. doi: https://doi.org/10.30506/jmee.2020.46442.